

Article

Aspergillus fumigatus Lytic Polysaccharide Monooxygenase AfLPMO9D: Biochemical Properties and Photoactivation of a Multi-Domain AA9 Enzyme

Pedro Ricardo Vieira Hamann ¹, Milena Moreira Vacilotto ¹, Fernando Segato ² and Igor Polikarpov ^{1,*}

¹ São Carlos Institute of Physics, University of São Paulo, Avenida Trabalhador São-Carlense, 400, Parque Arnold Schmidt, São Carlos 13566-590, SP, Brazil; pedrorvhamann@gmail.com (P.R.V.H.); milenamvacilotto@usp.br (M.M.V.)

² Synthetic and Molecular Biology Laboratory (SyMB), Department of Biotechnology, Lorena School of Engineering, University of São Paulo, Lorena 12602-810, SP, Brazil; segato@usp.br

* Correspondence: ipolikarpov@ifsc.usp.br

Abstract: Lytic polysaccharide monooxygenases (LPMOs) are critical players in enzymatic deconstruction of cellulose. A number of LPMOs have been identified at a genomics level; however, they still need to be characterized and validated for use in industrial processes aimed at cellulose deconstruction. In the present study, we biochemically characterized a new LPMO, a member of auxiliary activities family 9 (AA9) from the filamentous fungus *Aspergillus fumigatus* (AfLPMO9D). This LPMO demonstrated higher efficiency against amorphous cellulose as compared to more recalcitrant forms of cellulose such as bacterial cellulose and Avicel. AfLPMO9D has a capacity to oxidize the substrate at either the C₁ or C₄ positions, with pH-dependent regioselectivity. Photoactivation experiments demonstrated that light-stimulated chlorophyllin triggers AfLPMO9D activation without requirements of an external electron donor. AfLPMO9D is capable of boosting phosphoric acid-swollen cellulose depolymerization via GH7 endoglucanase and cellobiohydrolase. The results of the present study might help to elucidate the role of different LPMOs in cellulosic fiber deconstruction.

Keywords: lytic polysaccharides monooxygenases; AA9; cellulose; *Aspergillus fumigatus*



Citation: Hamann, P.R.V.; Vacilotto, M.M.; Segato, F.; Polikarpov, I. *Aspergillus fumigatus* Lytic Polysaccharide Monooxygenase AfLPMO9D: Biochemical Properties and Photoactivation of a Multi-Domain AA9 Enzyme. *Processes* **2023**, *11*, 3230. <https://doi.org/10.3390/pr11113230>

Academic Editor: Francisc Peter

Received: 19 October 2023

Revised: 12 November 2023

Accepted: 13 November 2023

Published: 16 November 2023



Copyright: © 2023 by the authors. Licensee MDPI, Basel, Switzerland. This article is an open access article distributed under the terms and conditions of the Creative Commons Attribution (CC BY) license (<https://creativecommons.org/licenses/by/4.0/>).

1. Introduction

The high prices of fossil fuels and the urgent need to develop new energy matrices with reduced greenhouse gas emissions have driven a search for the use of renewable sources, such as lignocellulosic residues [1]. One of the principal bottlenecks in using plant cell wall carbohydrates to produce renewable fuels is the inherent recalcitrance that arises from several factors, including the presence of microbial and enzyme inhibitors such as lignin [2] and the natural plant cell wall architecture that shields its cellulosic core with hemicellulose/lignin, barring the accessibility of enzymes and microorganisms [3].

In addition to the natural recalcitrance in plant cell wall organization, cellulose fibers have intrinsic recalcitrance [4]. The biochemical composition of cellulose is much simpler than that of other structural polysaccharides such as xylan, which is built by different sugars and contains side chains [5]. Cellulose, a β -1,4-D-glucopyranose homopolysaccharide with a degree of polymerization ranging from 100 to 20,000 [6], tightly associates in fibers, forming regions of high crystallinity and thus contributing to its resistance to enzymatic deconstruction [7].

Although the primary cellulose-degrading enzymatic repertoire has been investigated for more than 70 years [8], the development of cost-effective commercial enzymatic formulations for efficient cellulose deconstruction is still in progress [9]. The basic cellulose enzymatic degradation system comprises cellobiohydrolases, endo- β -1,4-glucanases, and β -glucosidases [7]. Briefly, cellulose is deconstructed by the action of endo- β -1,4-cellulase

(EC 3.2.1.4), which hydrolyzes the glycosidic bonds of amorphous regions, releasing short-chain cello-saccharides. Cellobiohydrolases hydrolyze the crystalline portion from the reducing (EC 3.2.1.176) and non-reducing (EC 3.2.1.91) termini of cellulosic fibers, releasing cellobiose. Finally, short-chain cello-oligosaccharides and cellobiose are further hydrolyzed to D-glucose by β -glucosidases (EC 3.2.1.21) [10].

More recently, other proteins with auxiliary activities have been identified as crucial enzymes in cellulose solubilization. Lytic polysaccharide monoxygenases (LPMOs), formerly known as fungal glycoside hydrolases of the family 61 (GH61), are copper-dependent enzymes with oxidative activity against cellulose [11]. LPMOs are categorized as Auxiliary Activity (AA) in the CAZy database [12], and those classified as AA9 are fungal LPMOs that are active in cellulose depolymerization. Oxidative cleavage of cellulose by lytic polysaccharide monoxygenases can occur at the C1 or C4 positions, generating lactones and 4-keto-sugars, respectively [13]. Currently, in addition to cellulose, LPMOs are known to be active against various carbohydrates, including chitin [14], xylan [15], and xyloglucan [16].

Apergillus fumigatus is a well-known opportunistic human pathogen [17]; however, more recently, it has been gaining biotechnological interest owing to its enzymatic arsenal for plant cell wall deconstruction [18]. Earlier, our research group characterized two AA9 *A. fumigatus* AA enzymes [19]. In the present study, a novel AA9 containing a cellulose-specific carbohydrate-binding module (CBM1), AfLPMO9D, was expressed in *A. nidulans*, purified, and characterized. Biochemical parameters, such as the optimal temperature and pH, were identified, and the LPMO specificity for different cellulosic substrates was determined. Aiming to elucidate the role of AfLPMO9D in cellulose deconstruction, its addition to monocomponent cellulases was evaluated. Moreover, a photoactivated system using chlorophyllin as a photosensitizer was employed to assess AfLPMO9D light-driven activation. The results of the present study will help us to understand the role of different LPMOs in cellulose deconstruction.

2. Material and Methods

2.1. Bioinformatic Analysis

The *A. fumigatus* AfLPMO9D nucleotide sequence was retrieved from NCBI GenBank using *A. fumigatus* AF293, locus tag AFUA_3G03870, and protein ID XP_748707.1. In addition, a mature protein sequence was obtained from the transcript Afu3g03870_mRNA deposited in MycoCosm [20]. Protein signal peptides were predicted using SignalP [21], and protein glycosylation sites were determined using NetOGlyc 4.0 and NetNGlyc 1.0 [22]. An initial search for similar proteins was conducted using the mature protein sequence in the NCBI Blastp (protein–protein database). Protein sequence alignment was performed using the ClustalW [23] program in Unipro UGENE 42.0 [24]. For protein alignment, sequences of already characterized LPMOs from *A. fumigatus* [19] and other organisms, HiLPMO9B *H. irregulare* [Uniprot:W4KMP1], LPMO9A-2 *G. trabeum* [Uniprot:A0A1C9ZMC5], cel61g AA9 *G. trabeum* [Uniprot:F8T947], LPMO9F *N. crassa* [Uniprot:Q6MGH2], eglD AA9 *A. nidulans* [Uniprot:Q5BCX8], LsAA9A *L. similis* [Uniprot:A0A0S2GKZ1], and LPMO9D *N. crassa* [Uniprot:Q1K8B6], were compared to AfLPMO9D; native signal peptides from proteins were removed after in silico prediction before proceeding to protein alignments. The three-dimensional model of the protein was predicted using AlphaFold [25], and protein visualization was performed using PyMOL 2.5 [26].

2.2. AfLPMO9D Cloning and Expression in *A. nidulans*

Cloning and selection of *A. nidulans* A773 transformants carrying AfLPMO9D under the control of the glucoamylase promoter were performed as previously reported [19]. The protein expression was performed in static conditions during tray cultivation. Briefly, *A. nidulans* transformants were cultivated in autoclaved (20 min, 121 °C 1.5 kgf/cm²) solid minimal medium composed of 1% (*w/v*) glucose, 1.5% (*w/v*) agar, 1 × minimal mineral solution, 1Xtrace element solution, and 1 mg/L pyridoxine for 48 h at 37 °C [27]. After fungal growth, three agar plates were used to inoculate 500 mL of filter-sterilized (0.22 μ m)

liquid induction medium composed of 1% (*w/v*) glucose, 3% (*w/v*) maltose, 1X minimal mineral solution, 1X trace elements solution, 1 mg/L pyridoxine, and pH adjusted to 6.5. The inoculated liquid medium was transferred to sterilized polypropylene trays and cultivated for 40 h at 37 °C.

Next, 1 L of culture supernatant was filtered through miracloth tissue (Merck Millipore, Darmstadt, Germany), centrifuged at 15,000× *g* at 4 °C for 30 min, and the clarified supernatant was further ten-fold concentrated in a 5 kDa hollow-fiber membrane. After concentration, the supernatant enriched with AfLPMO9D was analyzed using Coomassie blue-stained 12% SDS-PAGE [24] and stored at −20 °C until further purification.

2.3. AfLPMO9D Purification

The ten-fold concentrated supernatant enriched with AfLPMO9D was subjected to overnight 70% (NH₄)₂SO₄ precipitation, centrifuged at 15,000× *g* at 4 °C for 30 min, and the resulting protein pellet was resuspended in 50 mM Tris-HCl pH 8.0, with 1 M (NH₄)₂SO₄. Finally, the supernatant was applied to a hydrophobic interaction column (HiPrep Phenyl FF 16/10, GE Healthcare, Waukesha, WI, USA) pre-equilibrated in 50 mM Tris-HCl buffer pH 8.0 and 1 M (NH₄)₂SO₄, and protein was eluted in a descending (NH₄)₂SO₄ linear gradient. Fractions without ammonium sulfate containing the recombinant protein of interest were further collected and concentrated in a 10 kDa polyethersulfone membrane (GE Healthcare) [28,29]. The partially purified AfLPMO9D was further separated into a Superdex G75 column using 50 mM sodium acetate (pH 5) with 150 mM NaCl as the eluent, and the corresponding purified samples were analyzed using Coomassie blue-stained 12% SDS-PAGE. Chromatography was performed in an ÄKTA purifier (GE Healthcare) using a 1 mL/min flow rate, and protein elution was monitored by UV absorbance at 280 nm. Protein quantification was performed using a NanoDrop 2000 UV Visible spectrophotometer (Thermo Scientific, Waltham, MA, USA).

After purification, AfLPMO9D was three-fold saturated with CuSO₄ on a molar basis; to remove the excess copper, the purified protein was subjected to ultrafiltration in a 10 kDa polyethersulfone membrane. To eliminate possible contamination of *A. nidulans*' native cellulases, heat treatment was performed as previously reported by our research group [28], and *p*-nitrophenyl-β-D-cellobioside and *p*-nitrophenyl-β-D-glucoside were used as chromogenic substrates to evaluate cellulase contamination.

2.4. Soluble Products Detection by HPAEC

Soluble oligosaccharides were analyzed via high-performance anion exchange chromatography with pulsed amperometric detection (HPAEC-PAD), using a Dionex ICS-5000 system coupled with an ion exchange column CarboPAC PA1 (250 mm × 2 mm) (Thermo Scientific). A total of 100 mM NaOH (buffer A) and 500 mM sodium acetate with 100 mM NaOH (buffer B) were used as eluents, and the running conditions were as reported elsewhere [29]. Non-oxidized cello-oligosaccharides with degree of polymerization 1-6 (Sigma Aldrich, Darmstadt, Germany), glucuronic acid (Sigma Aldrich), and C1-oxidized cello-oligosaccharides (DP from 2 to 6, prepared as described in [30]) were used as standards. Prior to HPAEC-PAC analysis, reaction supernatant was filtered with the 0.22 μm CHROMAFIL Xtra PTFE-20/25 syringe filter (Macherey-Nagel, Düren, Germany) in order to separate the soluble products liberated by the LPMO from the insoluble substrate.

2.5. Specificity to Different Substrates

The enzymatic activity of AfLPMO9D was evaluated against different cellulosic substrates; briefly, reactions were carried out in 300 μL containing 1 μM of AfLPMO9D, 0.3% (*w/v*) cellulosic substrate, and 1 mM ascorbic acid, and the reactions were prepared in 50 mM sodium acetate pH 5.0 and performed for 16 h at 50 °C with 1000 rev·min^{−1} in a thermomixer (Eppendorf® ThermoMixer® C, Hamburg, Germany), similar to described elsewhere [29]. The final reaction was stopped by boiling at 95 °C for 5 min and centrifuging at 13,000× *g* for 10 min at room temperature. Supernatant was used for soluble

sugar detection analysis using HPAEC-PAD. The enzymatic reactions were performed in duplicate, and the control reactions used only the substrate or enzyme.

Cellulosic substrates, Avicel[®] PH-101 (Sigma Aldrich), phosphoric acid-swollen cellulose (PASC), and bacterial cellulose were mixed in deionized water before use in enzymatic assays. The filter paper was then cut into fine pieces and added to the final reaction. PASC was produced from Avicel[®] PH-101, according to a previously reported procedure [31], and bacterial cellulose, as described elsewhere [32].

2.6. Biochemical Characterization

To access effect of pH on AfLPMO9D oxidative activity, enzymatic assays were carried out as described above, replacing the buffer system with 50 mM citrate phosphate in a pH range from 3 to 8. The temperature effect was also carried out under standard enzymatic conditions using 50 mM sodium acetate (pH 5) and varying the temperature from 30 to 70 °C. The effects of different reducing agents were evaluated by replacing 1 mM ascorbic acid with 1 mM L-cysteine, glutathione, or pyrogallol (2,3-dihydroxy phenol). Biochemical characterization was performed using PASC as a standard substrate, and the results are reported with standard deviation from two independent experiments. Soluble sugars were analyzed using HPAEC-PAD, and peaks of cello-oligosaccharides of interest were integrated into the chromatograms (nC·min) and summed up in order to allow a more direct comparison of the data. This approach was used to study several C₁-C₄-oxidized LPMOs [28,33].

2.7. Light-Driven Activation

The light-mediated oxidative activity of AfLPMO9D was evaluated against PASC following standard enzymatic assays at pH 7 using 50 mM citrate phosphate buffer. The light-activated reactions were performed in two different experimental sets. First, 1 mM chlorophyllin was utilized to replace the reducing agent ascorbic acid, and the second set of experiments used both the reducing agent and chlorophyllin. Control reactions consisted of using 1 mM chlorophyllin in the absence of light and performing light activation using 1 µM LPMO9H as an enzyme model, previously reported to be activated by light [28]. Light-activated reactions were performed in a dark room with an unsealed thermomixer; a red LED light was directly applied above the reaction tubes (2 mL colorless polypropylene tubes, Eppendorf Tubes[®], Hamburg, Germany) with an average photon irradiance of 220.8 µmol photons·s⁻¹·m⁻².

2.8. Cellulose Hydrolysis

PASC and Avicel hydrolysis were performed by adding AfLPMO9D to different cellulases. Briefly, 1 µM or 0.1 µM of AfLPMO9D was added to 10 µg of cellobiohydrolase (GH7 CBHI from *Trichoderma reesei*) or endoglucanase (GH7 endo-β-1,4-cellulase from *Thielavia terrestris*) in a 300 µL reaction containing Avicel or PASC (0.3% w/v). Reactions were prepared in 50 mM sodium acetate pH 5.0 with 1 mM Asc and carried out at 50 °C for 24 h at 1000 rev·min⁻¹ in a thermomixer (Eppendorf[®] ThermoMixer[®] C). After hydrolysis, the reactions were boiled at 95 °C for 5 min, and the total reducing sugar content was determined using the 3,5-dinitro salicylic acid method [34] employing a glucose standard curve.

3. Results and Discussion

3.1. Protein Sequence Alignment and Heterologous Expression

Nowadays, lytic polysaccharide monoxygenase genes with an active role in plant carbohydrates deconstruction have been annotated for several microorganisms. In this category of enzymes with auxiliary activity, those of fungal origin classified as AA9 family are the most studied for cellulose deconstruction processes [35,36]. A search of the AfLPMO9D protein sequence against protein databases revealed its high identity (>90%) with proteins of *Aspergillus* species closely related to *A. fumigatus* [37], including *As-*

pegillus fischeri (90.52% identity, XP_001259147.1), *Aspergillus fumigatiaffinis* (89.91% identity, KAF4251698.1), and *Aspergillus lentulus* (90.21% identity, GAQ04932.1).

AfLPMO9D showed only high similarity with proteins of *Aspergillus* species in the *Fumigati*, and none of these proteins have been validated and annotated as glycosyl hydrolase GH61 or putative endo- β -1,4-glycosidases. Indeed, only *A. fumigatus* has been explored as a source of plant cell wall-degrading enzymes; other related species have only been studied with a focus on their human pathogenicity traits [38].

Protein alignment with characterized LPMOs displayed the two conserved histidines that are typical for the catalytic domain of LPMOs (Supplementary Figure S1). In addition to the AA9 catalytic domain, AfLPMO9D harbors a C-terminal cellulose-specific carbohydrate-binding module from family 1, which is typically found in cellulases and other LPMOs [28] (Supplementary Figure S1c,d). Although in silico modeling of AfLPMO9D could result in a structure similar to other LPMOs, the positioning of the CBM 1 domain was closely associated with the AA9 domain of the LPMO, probably due to hydrophobic interactions which biased the in silico protein structure prediction. Indeed, previous studies employing small-angle X-ray scattering models have demonstrated the flexibility of linker regions in multi-domain LPMOs [28].

AfLPMO9D was successfully expressed and secreted into the culture media upon induction by *A. nidulans* carrying the full-length gene sequence coding for the protein under the α -glucosidase promoter. Although the primary protein sequence results in a predicted molecular weight of 33.22 kDa, after protein expression, a higher molecular weight was observed, ~45 kDa (Supplementary Figure S2). These results are aligned with other eukaryotic LPMOs heterologously expressed in eukaryotic hosts, such as *Pichia pastoris* and [39] *A. nidulans* [19]. The prediction of *N*- and *O*-glycosylation indicated 38 putative *O*-glycosylation and two *N*, which might explain the discrepancy between the observed and predicted molecular weights of AfLPMO9D. Furthermore, the expression of AfLPMO9D in a phylogenetically related eukaryotic system as a host organism must contribute to more accurate post-translational modifications; for instance, eukaryotic LPMOs have their *N*-terminal copper coordinating histidine methylated, which protects the protein against oxidative damage [40].

3.2. AfLPMO9D Specificity for Different Cellulosic Substrates

After protein purification and thermal treatment to remove native *A. nidulans* cellulases, AfLPMO9D was screened for oxidative activity against Avicel, PASC, filter paper, and bacterial cellulose. AfLPMO9D was capable of cleaving all the investigated substrates by employing C_1 and C_4 oxidation, generating either C_1 , C_4 , or C_1 – C_4 , and non-oxidized products (Figure 1). Although the enzyme could oxidize different cellulose-based substrates, it displayed contrasting efficiency against cellulosic substrates with higher crystallinity. For instance, products obtained from PASC enzymatic oxidation were almost five-fold higher than those generated using bacterial cellulose and Avicel as substrates.

Some lytic polysaccharide monooxygenases are reported to be very active against cellulosic substrates with a high crystallinity [41,42]; however, the present report shows that AfLPMO9D displays better efficiency against a non-crystalline substrate, namely, PASC. Recently, it has been reported that *Thermothielavioides terrestris* possesses different AA enzymes with a distinctive role in cellulose-based material deconstruction. For example, TtLPMO9A displayed the highest activity against PASC compared to Avicel and pulp fibers [43]. For *A. fumigatus*, two other AA9s have been fully characterized [19], and they displayed at least a five-fold difference in their oxidative activity against Avicel. These reports, along with the data presented in this study, highlight that *A. fumigatus* has AA9s specialized in cellulosic substrates with diverging crystallinity. This strategy may enhance the cellulose deconstruction and therefore facilitate lignocellulose colonization by fungi.

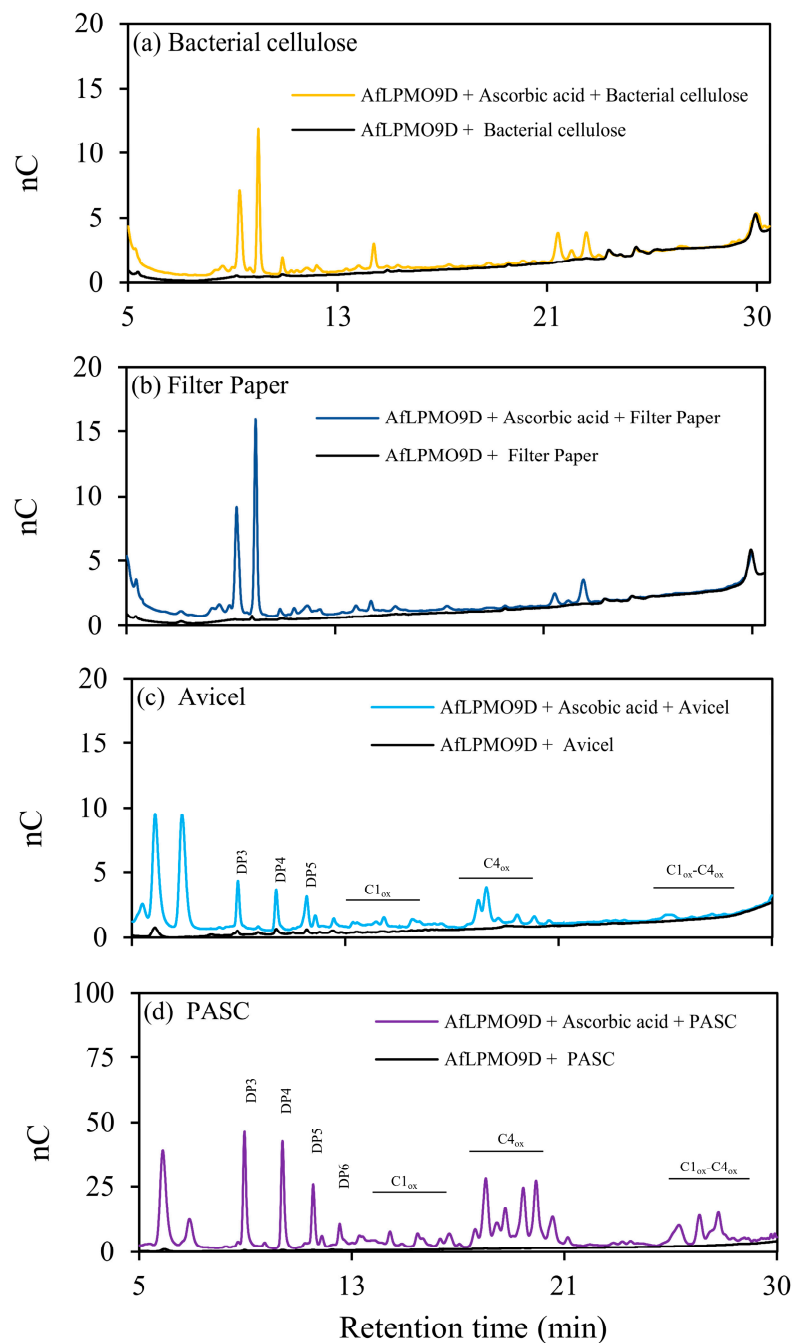


Figure 1. HPAEC-PAD chromatogram profile of soluble products released by 1 μM AfLPMO9D after activity against 0.3% (*w/v*). Samples were incubated with 50 mM sodium acetate buffer pH 5.0 and 1 mM Asc and maintained at 50 $^{\circ}\text{C}$ and 1000 $\text{rev}\cdot\text{min}^{-1}$ for 16 h. Control reactions (black lines) were performed in the absence of a reductant.

3.3. AfLPMO9D Biochemical Properties

3.3.1. pH Effect

The effect of pH on AfLPMO9D activity was demonstrated over a broad pH range, with maximum activity at pH 7 and 8. At pH 5, which is typically employed in cellulose hydrolysis by fungal enzymes, the enzyme exhibited >50% of its maximum activity (Figure 2). The effect of pH also revealed a particular effect on the type of cello-oligosaccharides released upon enzymatic oxidation. For non-oxidated and C_1 – C_4 oxidized cello-oligosaccharides, there is a linear increment from the acidic to the basic pH range; on

the other hand, peak C₄ oxidizing activity occurs at pH 5 and sharply decreases at a neutral pH (Figure 3).

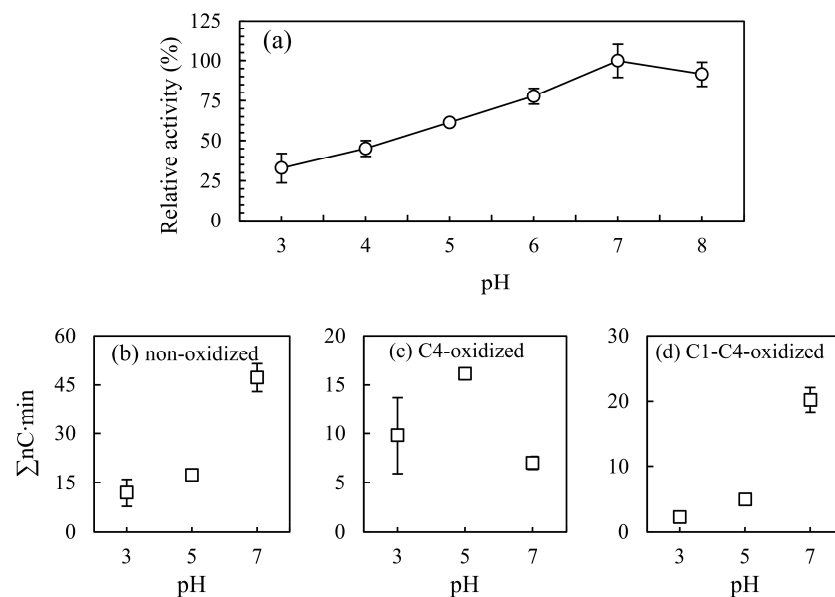


Figure 2. (a) pH effect on AflPMO9D oxidative activity against 0.3%(w/v) PASC using 1 mM ascorbic acid as a reducing agent; (b) total non-oxidized, (c) C₄-oxidized, and (d) C₁-C₄-oxidized. Samples were analyzed using HPAEC-PAD, and peak areas (nC·min) were summed for non-oxidized, C₄-oxidized and/or C₁-C₄-oxidized cello-saccharides. Relative activity was calculated based on the total amount of soluble sugars released by the enzyme under different pH conditions. Vertical bars represent the standard deviation from two separate experiments. Reactions were incubated at 50 °C and 1000 rev·min⁻¹ for 16 h with 1 μM LPMO in 50 mM citrate phosphate buffer (pHs from 3.0 to 8.0).

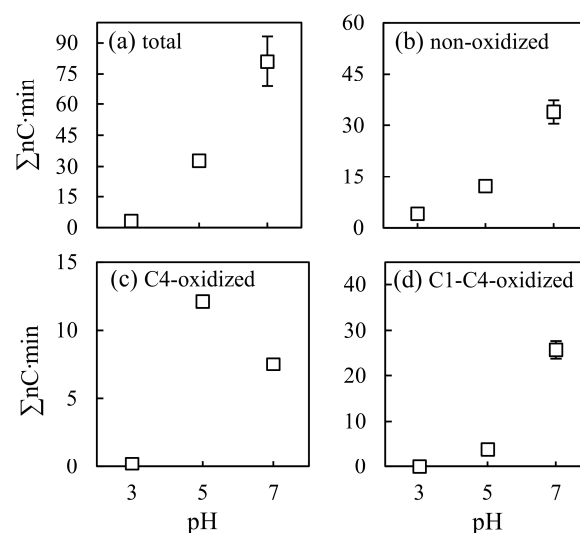


Figure 3. pH effect in AflPMO9D oxidative activity against 0.3%(w/v) PASC using 1 mM pyrogallol as a reducing agent. (a) Total products released, (b) total non-oxidized, (c) C₄-oxidized, and (d) C₁-C₄-oxidized. Samples were analyzed using HPAEC-PAD, and peak areas (nC·min) were summed for non-oxidized, C₄-oxidized and/or C₁-C₄-oxidized cello-saccharides. Relative activity was calculated based on the total amount of soluble sugars released by the enzyme under different pH condition. Vertical bars represent the standard deviation from two separate experiments. Reactions were incubated at 50 °C and 1000 rev·min⁻¹ for 16 h with 1 μM LPMO in 50 mM citrate phosphate buffer (pHs from 3.0 to 7.0).

The pH effect reported in the present study diverges from the results previously reported for AfAA9B and AfAA9A, two AA9 from *A. fumigatus* [19]. The two previously characterized enzymes displayed their maximum activity at pH 8, and at pH 7, 60% of the maximum activity was observed. AfAA9B and AfAA9A display only significant activity at pH 6 in the acidic pH range, whereas AfLPMO9D consistently displayed >25% of its maximum activity in this range. AfLPMO9D displays activity over a broad pH range, suggesting that this enzyme could be incorporated into commercially available cellulase blends, primarily active at pH 5, without the drawbacks of pH inactivation. The broader pH range observed for AfLPMO9D can be a direct consequence of its inherent reduced activity, which might decrease oxidative damage, allowing the enzyme to work further under sub-optimal conditions.

To evaluate whether there was a correlation between the reducing agent used, ascorbic acid, and the effect of pH on the oxidative activity of AfLPMO9D, the same experiment was conducted using pyrogallol (2,3-dihydroxy phenol) as a reducing agent. The results demonstrated that, at least for AfLPMO9D, the use of either pyrogallol or ascorbic acid did not alter the effect of pH on the enzymatic activity (Figure 3). In addition, the rate of non-oxidized and C₁–C₄-oxidized products prevailed, as seen for the pH effect using ascorbic acid as a reducing agent.

Golten and colleagues [44] demonstrated that the pH impacts the ionization state of reductants and, consequently, their reactivity with the LPMO and in situ production of H₂O₂. Ascorbic acid (AscH₂), for instance, is predominantly in its ascorbate form (AscH[−]) between pHs from 5 to 11 (pK_{a1} and pK_{a2} equal to 4.1 and 11.6, respectively). The reaction with AscH[−] and O₂ + Cu(II) was shown to be faster than with AscH₂ [45], which implies a faster H₂O₂ production in the system as the pH of the medium moves away from 5 and approaches 11. Similarly, pyrogallol (pK_a equal to 9.05) presents an increase in the oxidation rates [46] and H₂O₂ production [47] with increasing pH. In view of that, the higher LPMO catalytic activity observed in alkaline pHs might correspond to an increase in hydrogen peroxide generation.

The detailed mechanism by which C₁/C₄ LPMOs regioselectively oxidize C₁ or C₄ termini has not been fully elucidated. However, there is evidence that the position of aromatic amino acids on the LPMOs surface may lead to different binding to the substrate, leading to differential regioselectivity [48]. Similarly, reports have indicated that acidic amino acids on the surface of LPMOs might help hydrogen bond cellulosic fibers, thus directing enzyme regioselectivity [49].

Observing the AfLPMO9D structure, three negatively charged amino acids are exposed at the protein surface close to the two copper-coordinating histidines, Asp₄₇ (15.7 Å), Asp₂₀ (15.8 Å), and Asp₈₄ (13.3 Å). These amino acid positions could not explain the pH dependence in C₁ and C₁–C₄ oxidation observed in the present study because in the pH range where more C₄ oxidized termini are present, acidic side chain amino acids are already fully deprotonated. However, a search of the AfLPMO9D surface for charged and polar amino acids resulted in His₁₆₄ (8.3 Å) (Supplementary File S3). Although histidines are rarely reported as coordinating the enzymes binding to cellulose, previous studies showing the replacement of aromatic residues in carbohydrate-binding modules by histidines have demonstrated that the His side chain may coordinate cellulose binding when placed in more alkali pH conditions [50], when histidine residues assume a partial negative charge. In summary, the proximity of histidine groups in conjunction with previously reported acidic amino acids may possibly contribute to the regioselective pH dependence, as observed in the present study.

3.3.2. Effect of Temperature

AfLPMO9D could perform PASC oxidation in a broad temperature range (Figure 4), displaying peak activity from 30 to 40 °C and a slight decrease of approximately 20% in a temperature range from 40 to 60 °C. On the other hand, a sharp activity decrease was observed in temperatures above 60 °C. Compared to other LPMOs, AfLPMO9D displayed

a broader temperature range than TausLPMO9B (AA9) from *Thielavia australiensis* [51]. The temperature effect observed in the present study is similar to that of AfAA9, a C₁ oxidizing LPMO from *A. fumigatus* [19].

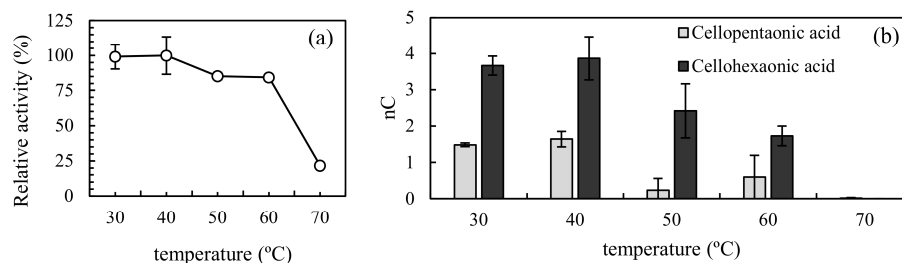


Figure 4. (a) Temperature effect on AfLPMO9D activity against 0.3% (w/v) PASC using 1 mM ascorbic acid as a reducing agent. Samples were analyzed using HPAEC-PAD, and relative activity was calculated based on the total amount of soluble sugars released by the enzyme under different temperature conditions. (b) Temperature-dependent cellopentaonic and cellohexaonic acid production. Vertical bars represent the standard deviation from two separate experiments. Reactions were incubated at 1000 rev·min⁻¹ for 16 h with 1 μM LPMO in 50 mM sodium acetate buffer pH 5.0.

Although peak activity was observed between 30 and 50 °C, the diversity of the released oxidized products was temperature-dependent, with cellohexaonic and cellopentaonic acids being the most abundant (Figure 4b). The major release of cellohexaonic and cellopentaonic acids was observed between 40 and 50 °C. These products consistently decreased beyond this temperature range and were therefore less abundant. Altogether, the pH effect and temperature range may indicate that this enzyme is relevant to the development of cellulose blends with the potential for formulation, aiming at simultaneous saccharification and fermentation [52]. In this process, lower temperatures can be employed to deconstruct cellulose, and pH shifts are prone to occur during cellulose deconstruction and fermentation.

3.4. Effect of Different Reducing Agents

For LPMOs to effectively achieve carbohydrate oxidation, molecular oxygen and a reducing agent may be required to act as electron donors. In our screening of reducing agents, relevant biological compounds, such as the amino acid L-cysteine, glutathione, pyrogallol, and ascorbic acid, were tested (Figure 5). In summary, glutathione, pyrogallol, and ascorbic acid resulted in the same levels of oxidized sugars, whereas only 30% of the maximum observed was detected when employing L-cysteine as an electron donor.

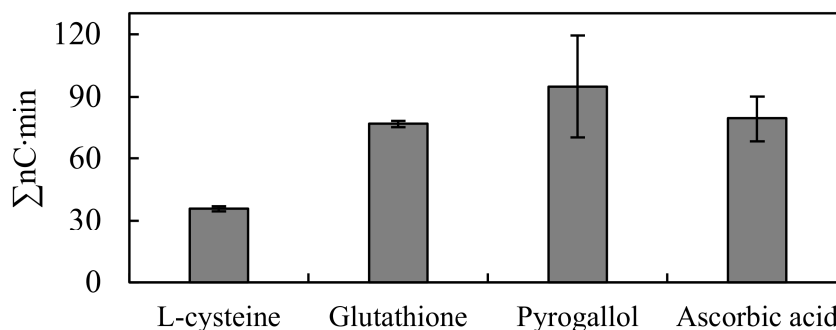


Figure 5. Effect of different reducing agents, at 1 mM, as electron donor for 1 μM AfLPMO9D during 0.3% (w/v) PASC oxidation. Reactions were incubated in 50 mM sodium acetate buffer pH 5.0 for 16 h at 50 °C and 1000 rev·min⁻¹. Vertical bars represent the standard deviation from two independent experiments. Blanks were performed in the absence of a reducing agent. Samples were analyzed using HPAEC-PAD, and peak areas (nC·min) were summed for non-oxidized, C₄-oxidized, and C₁–C₄-oxidized cello-oligosaccharides.

The divergent effect observed for L-cysteine and glutathione (cysteine, glutamic acid, and glycine) was not expected; hence, they are both sulfur-containing groups and, more specifically, a sulfhydryl group with a strong basic pKa. This difference may be due to the antioxidative role of glutathione, one of the most studied biological antioxidants [53], which may protect LPMO from further oxidative damage from excess peroxide generated during the oxidative cleavage of PASC, an event known as auto-oxidation inactivation [40].

Despite the significant results obtained using glutathione, and to a lesser extent, for L-cysteine, in industrial conditions for the application of LPMOs, it is not feasible to use such compounds as electron donors, mainly because of their cost and availability, which could reduce the economic viability of the process. On the other hand, LPMOs may use inexpensive and widely available electron donors derived from lignocellulosic biomass, such as phenolic compounds such as gallic acid, for example [33]. In this respect, pyrogallol, a tannic acid-derived phenol, can be employed as a reducing agent for AfLPMO9D, generating the same level of oxidized sugars when employing ascorbic acid as an electron donor, a model molecule for studying LPMOs. The possibility of using phenolic compounds derived from plant cell walls [54] demonstrates the versatility of electron donors for LPMOs. Similarly, in natural environments, it is expected that lignin and related compounds might work as electron donors for enzymatic oxidation of plant carbohydrates.

3.5. Light-Driven Activation of AfLPMO9D

In addition to the oxidative activity of LPMOs, this enzyme class can perform the oxidative cleavage of carbohydrates by employing natural peroxygenase activity, for example, H_2O_2 as a co-substrate [55,56]. Assuming their capacity to consume peroxide, LPMOs can be activated by a system that can autonomously produce peroxide and electrons to reduce the enzyme's catalytic copper, thereby activating the oxidative cleavage of carbohydrates. In this respect, we demonstrated that light-derived excitation of the photosensitizer chlorophyllin could activate AfLPMO9D (Figure 6). The results demonstrated that light excitation could trigger the activation of LPMO, generating oxidized and non-oxidized products, as observed for ascorbic acid-supplemented reactions. The co-addition of ascorbic acid and chlorophyllin in a light-driven reaction did not further boost the PASC deconstruction (Figure 6c).

The mechanism underlying the light-driven reaction of LPMO is debatable, and is not fully understood [57,58]. However, in the absence of an external electron donor and light excitation, chlorophyllin alone cannot trigger the oxidative cleavage of PASC by AfLPMO9D. In other words, the excitation caused by light leads to peroxide production and other oxygen-reactive species, and AfLPMO9D will be used as a co-substrate in the oxidative cleavage of PASC. Indeed, it was shown that the addition of nM concentrations of superoxide dismutase (SOD), that converts $O^{\bullet-}$ to H_2O_2 , increases the LPMO activity, whereas μ M concentrations of SOD results in enzymatic oxidative damage due to an excess of hydrogen peroxide [59,60]; this suggests a role of radical superoxide as a reducing agent for LPMOs. Another reasonable explanation for the light-driven activation of LPMO might be the direct transfer of the redox potential from the photosensitizer to the enzyme [57,59].

Employment of the reducing agent, ascorbic acid, and light did not result in an additive effect after 16 h of incubation; this may have resulted from the formation of excess reactive species, leading to oxidative damage, as previously observed by Bissaro and colleagues [59]. The said work demonstrated that Chl/light-Asc LPMO fueled reactions present higher initial catalytic rates when compared to those supplemented with only Chl/light or Asc, but the accumulation of H_2O_2 early on produced by both Chl/light and Asc led to fast inactivation of the enzyme.

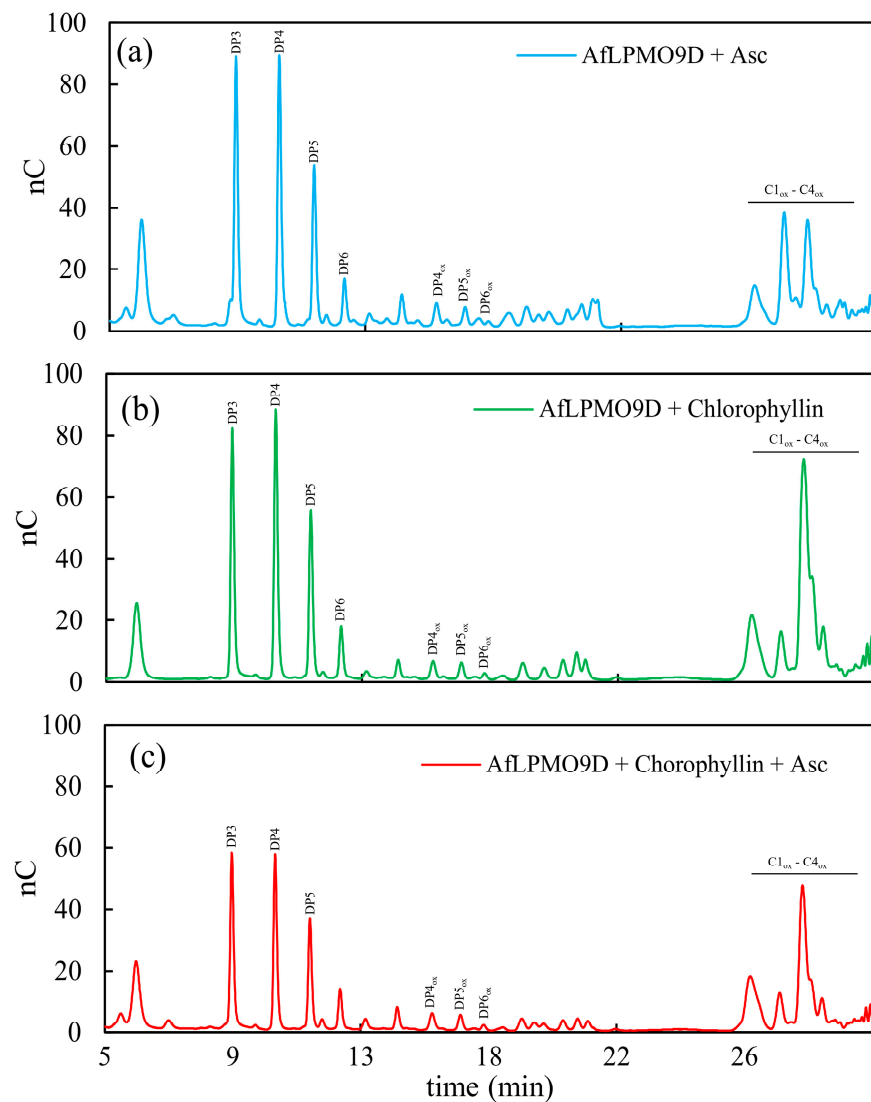


Figure 6. HPAEC-PAD chromatogram profile of soluble products from photoactivation of 1 μM AfLPMO9D by 1 mM chlorophyllin, using 0.3% (w/v) PASC as substrate. (a) AfLPMO9D reaction in the presence of 1 mM ascorbic acid and absence of photoactivation (red light, $220.8 \mu\text{mol photons}\cdot\text{s}^{-1}\cdot\text{m}^{-2}$), (b) reaction in the absence of reducing agent and presence of light and chlorophyllin, and (c) combined effect of photo-activated reaction and presence of reducing agent. Samples were incubated in 50 mM citrate phosphate buffer pH 7.0 for 16 h at 50°C and $1000 \text{ rev}\cdot\text{min}^{-1}$.

Furthermore, more recent studies have shown that lignin [54] and redox compounds present in insect exoskeletons [61] are able to drive LPMO reactions when exposed to visible light, which contributes to plant cell wall and insect cuticles degradation. In summary, the light activation of LPMO may represent a novel, feasible, and cost-effective strategy to boost plant cell wall depolymerization and, consequently, promote a revalorization of the biomass.

3.6. Supplementation of Glycoside Hydrolases with AfLPMO9D

Since the initial reports regarding the oxidative activity of LPMOs against cellulose, there is common knowledge about its boosting potential in cellulose hydrolysis [62,63]. In the present study, an improvement in hydrolysis of PASC was observed when supplementing cellobiohydrolase I and endoglucanase, both of the GH7 family, with AfLPMO9D (Figure 7a,b). For both enzymes, maximum enhancement was obtained using 1 μM of AfLPMO9D, obtaining $26.80 \mu\text{g}/\text{mL}$ of reducing sugar with endoglucanase and $45.48 \mu\text{g}/\text{mL}$

combining endoglucanase with AfLPMO9D. In contrast, cellobiohydrolase I generated 11.01 $\mu\text{g}/\text{mL}$ of reducing sugar; when supplemented with AfLPMO9D, 26.01 $\mu\text{g}/\text{mL}$ was obtained. Despite the significant improvement observed when employing PASC as the cellulosic substrate, no improvement was observed when cellobiohydrolase I was combined with AfLPMO9D for Avicel hydrolysis.

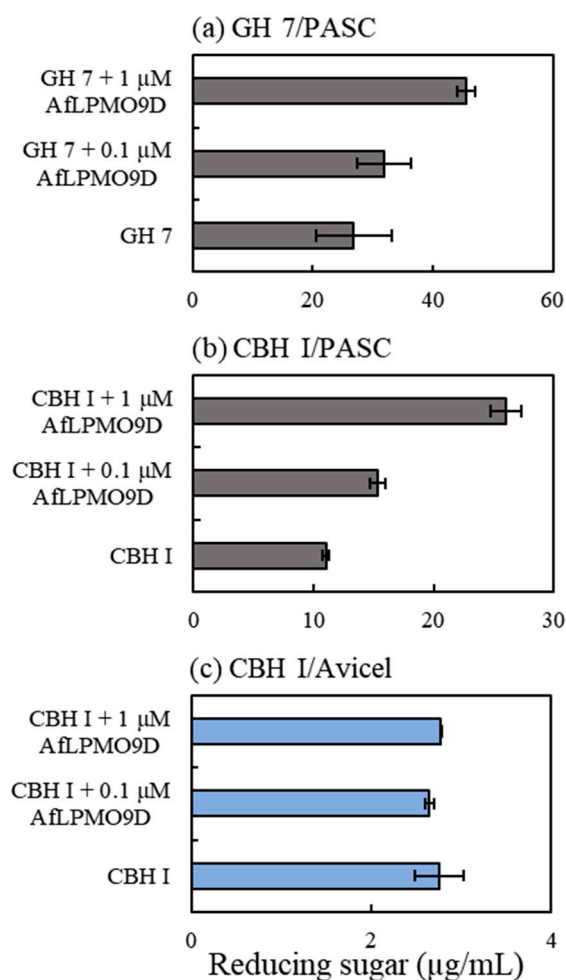


Figure 7. Effect of 1 μM or 0.1 μM AfLPMO9D addition to 10 μg of (a) endoglucanase and (b) cellobiohydrolase I, against 0.3%(w/v) PASC, and to (c) cellobiohydrolase I against 0.3%(w/v) Avicel. Narrow bars represent the standard deviation from two separate experiments. Grey and blue bars represent experiments carried out against PASC and Avicel, respectively. Reactions were carried out in 50 mM sodium acetate buffer pH 5.0 and 1 mM ascorbic acid and maintained at 50 $^{\circ}\text{C}$ for 24 h at 1000 $\text{rev}\cdot\text{min}^{-1}$. Supernatant was used for reducing sugar determination by the DNS method.

The results obtained when supplementing cellulases with AfLPMO9D indicated that this enzyme performs better against amorphous cellulosic substrates, corroborating our initial screening against substrates with distinct crystallinity levels, on which LPMO was primarily active against PASC (Figure 7). Previous studies have demonstrated that LPMO synergism with cellulase is substrate- and LPMO-dependent; for instance, it has been shown that the LPMO TtAA9E from *Thielavia terrestris* does not show synergism with *Trichoderma reesei* Cel7A, whereas LsAA9A from *Lentinus similis* has significant synergism during PASC hydrolysis [62], and *Thermothelomyces thermophilus* TtLPMO9H has been shown to perform best when combined with GH7 endoglucanase [28]. Furthermore, the lack of enhancement while combining the cellobiohydrolase and LPMO may be a consequence of protein diffusion in the reaction; since both enzymes harbor a cellulose-specific CBM, they

might be immobilized in different regions of cellulosic fiber, limiting their joint efficiency against insoluble substrates.

4. Conclusions

AfLPMO9D was expressed in *A. nidulans* and displayed oxidative activity against several cellulosic substrates, particularly amorphous cellulose. The broad pH range and temperature at which the highest activity is observed may make AfLPMO9D appealing for incorporation into new cellulase blends for cellulosic ethanol production. The enzyme was particularly active on amorphous cellulose and demonstrated synergy with cellobiohydrolase and endoglucanase from the GH7 family. Light-driven activation of the LPMO was observed. Although light-boosted enzymatic oxidation of cellulose is still not fully understood, our results demonstrated its potential for increasing the cellulose deconstruction efficiency.

Supplementary Materials: The supporting information can be downloaded at: <https://www.mdpi.com/article/10.3390/pr11113230/s1>.

Author Contributions: P.R.V.H.: manuscript writing, experiments execution, and design. M.M.V.: experiments execution, and design. F.S.: grant acquisition, and experiment design. I.P.: grant acquisition, experiments design, and manuscript witting. All authors have read and agreed to the published version of the manuscript.

Funding: This research was funded by research grants from Universidade de São Paulo—Brazil, and FAPESP (Fundação de Amparo à Pesquisa do Estado de São Paulo), grant numbers 2015/13684-0 and 2021/08780-1. Pedro R.V. Hamann received grants from FAPESP, grant numbers 2021/13009-2 and 2023/07897-8. Igor Polikarpov is a recipient of CNPq (Conselho Nacional de Desenvolvimento Científico e Tecnológico) grants 306852/2021-7 and 440180/2022-8. Milena M. Vacilotto was a recipient of CAPES (Coordenação de Aperfeiçoamento de Pessoal de Nível Superior) master's degree scholarship, grant number 88887.601517/2021-00.

Data Availability Statement: Data are contained within the article.

Conflicts of Interest: The authors declare no conflict of interest.

References

1. Cherubini, F. The biorefinery concept: Using biomass instead of oil for producing energy and chemicals. *Energy Convers. Manag.* **2010**, *51*, 1412–1421. [[CrossRef](#)]
2. Duarte, G.C.; Moreira, L.R.S.; Jaramillo, P.M.D.; Filho, E.X.F. Biomass-Derived Inhibitors of Holocellulases. *BioEnergy Res.* **2012**, *5*, 768–777. [[CrossRef](#)]
3. Brodeur, G.; Yau, E.; Badal, K.; Collier, J.; Ramachandran, K.B.; Ramakrishnan, S. Chemical and Physicochemical Pretreatment of Lignocellulosic Biomass: A Review. *Enzym. Res.* **2011**, *2011*, e787532. [[CrossRef](#)]
4. Kim, S.; Baek, S.-H.; Lee, K.; Hahn, J.-S. Cellulosic ethanol production using a yeast consortium displaying a minicellulosome and β -glucosidase. *Microb. Cell Fact.* **2013**, *12*, 14. [[CrossRef](#)] [[PubMed](#)]
5. Bastawde, K.B. Xylan structure, microbial xylanases, and their mode of action. *World J. Microbiol. Biotechnol.* **1992**, *8*, 353–368. [[CrossRef](#)] [[PubMed](#)]
6. Zhang, Y.-H.P.; Lynd, L.R. Determination of the Number-Average Degree of Polymerization of Cellodextrins and Cellulose with Application to Enzymatic Hydrolysis. *Biomacromolecules* **2005**, *6*, 1510–1515. [[CrossRef](#)] [[PubMed](#)]
7. Mansfield, S.D.; Meder, R. Cellulose hydrolysis—The role of monocomponent cellulases in crystalline cellulose degradation. *Cellulose* **2003**, *10*, 159–169. [[CrossRef](#)]
8. Bischof, R.H.; Ramoni, J.; Seiboth, B. Cellulases and beyond: The first 70 years of the enzyme producer *Trichoderma reesei*. *Microb. Cell Factories* **2016**, *15*, 106. [[CrossRef](#)]
9. Lopes, A.M.; Ferreira Filho, E.X.; Moreira, L.R.S. An update on enzymatic cocktails for lignocellulose breakdown. *J. Appl. Microbiol.* **2018**, *125*, 632–645. [[CrossRef](#)]
10. Sharma, A.; Tewari, R.; Rana, S.S.; Soni, R.; Soni, S.K. Cellulases: Classification, Methods of Determination and Industrial Applications. *Appl. Biochem. Biotechnol.* **2016**, *179*, 1346–1380. [[CrossRef](#)]
11. Morgenstern, I.; Powlowski, J.; Tsang, A. Fungal cellulose degradation by oxidative enzymes: From dysfunctional GH61 family to powerful lytic polysaccharide monoxygenase family. *Briefings Funct. Genom.* **2014**, *13*, 471–481. [[CrossRef](#)] [[PubMed](#)]

12. Terrapon, N.; Lombard, V.; Drula, E.; Coutinho, P.M.; Henrissat, B. The CAZy Database/the Carbohydrate-Active Enzyme (CAZy) Database: Principles and Usage Guidelines. In *A Practical Guide to Using Glycomics Databases*; Springer: Tokyo, Japan, 2017; pp. 117–131. [[CrossRef](#)]
13. Westereng, B.; Arntzen, M.; Aachmann, F.L.; Várnai, A.; Eijsink, V.G.; Agger, J.W. Simultaneous analysis of C1 and C4 oxidized oligosaccharides, the products of lytic polysaccharide monoxygenases acting on cellulose. *J. Chromatogr. A* **2016**, *1445*, 46–54. [[CrossRef](#)] [[PubMed](#)]
14. Hamre, A.G.; Eide, K.B.; Wold, H.H.; Sørli, M. Activation of enzymatic chitin degradation by a lytic polysaccharide monoxygenase. *Carbohydr. Res.* **2015**, *407*, 166–169. [[CrossRef](#)] [[PubMed](#)]
15. Frommhagen, M.; Sforza, S.; Westphal, A.H.; Visser, J.; A Hinz, S.W.; Koetsier, M.J.; van Berkel, W.J.H.; Gruppen, H.; A Kabel, M. Discovery of the combined oxidative cleavage of plant xylan and cellulose by a new fungal polysaccharide monoxygenase. *Biotechnol. Biofuels* **2015**, *8*, 101. [[CrossRef](#)]
16. Agger, J.W.; Isaksen, T.; Várnai, A.; Vidal-Melgosa, S.; Willats, W.G.T.; Ludwig, R.; Horn, S.J.; Eijsink, V.G.H.; Westereng, B. Discovery of LPMO activity on hemicelluloses shows the importance of oxidative processes in plant cell wall degradation. *Proc. Natl. Acad. Sci. USA* **2014**, *111*, 6287–6292. [[CrossRef](#)] [[PubMed](#)]
17. Latgé, J.-P. The pathobiology of *Aspergillus fumigatus*. *Trends Microbiol.* **2001**, *9*, 382–389. [[CrossRef](#)]
18. Saroj, P.; Manasa, P.; Narasimhulu, K. Biochemical Characterization of Thermostable Carboxymethyl Cellulase and β -Glucosidase from *Aspergillus fumigatus* JCM 10253. *Appl. Biochem. Biotechnol.* **2022**, *194*, 2503–2527. [[CrossRef](#)]
19. Velasco, J.; Pellegrini, V.d.O.A.; Sepulchro, A.G.V.; Kadowaki, M.A.S.; Santo, M.C.E.; Polikarpov, I.; Segato, F. Comparative analysis of two recombinant LPMOs from *Aspergillus fumigatus* and their effects on sugarcane bagasse saccharification. *Enzym. Microb. Technol.* **2021**, *144*, 109746. [[CrossRef](#)]
20. Grigoriev, I.V.; Nikitin, R.; Haridas, S.; Kuo, A.; Ohm, R.; Otilar, R.; Riley, R.; Salamov, A.; Zhao, X.; Korzeniewski, F.; et al. MycoCosm portal: Gearing up for 1000 fungal genomes. *Nucleic Acids Res.* **2014**, *42*, D699–D704. [[CrossRef](#)]
21. Nielsen, H. Predicting secretory proteins with SignalP. In *Protein Function Prediction*; Kihara, D., Ed.; Humana Press: New York, NY, USA, 2017; pp. 59–73. [[CrossRef](#)]
22. E Hansen, J.; Lund, O.; Tolstrup, N.; A Gooley, A.; Williams, K.L.; Brunak, S. NetOglyc: Prediction of mucin type O-glycosylation sites based on sequence context and surface accessibility. *Glycoconj. J.* **1998**, *15*, 115–130. [[CrossRef](#)]
23. Larkin, M.A.; Blackshields, G.; Brown, N.P.; Chenna, R.; McGettigan, P.A.; McWilliam, H.; Valentin, F.; Wallace, I.M.; Wilm, A.; Lopez, R.; et al. Clustal W and Clustal X version 2.0. *Bioinformatics* **2007**, *23*, 2947–2948. [[CrossRef](#)]
24. Okonechnikov, K.; Golosova, O.; Fursov, M.; The UGENE Team. Unipro UGENE: A unified bioinformatics toolkit. *Bioinformatics* **2012**, *28*, 1166–1167. [[CrossRef](#)] [[PubMed](#)]
25. Jumper, J.; Evans, R.; Pritzel, A.; Green, T.; Figurnov, M.; Ronneberger, O.; Tunyasuvunakool, K.; Bates, R.; Žídek, A.; Potapenko, A.; et al. Highly accurate protein structure prediction with AlphaFold. *Nature* **2021**, *596*, 583–589. [[CrossRef](#)] [[PubMed](#)]
26. Schrödinger, LLC. *The {PyMOL} Molecular Graphics System, Version~1.8*; Schrödinger, LLC.: New York, NY, USA, 2015.
27. Segato, F.; Damásio, A.R.; Gonçalves, T.A.; de Lucas, R.C.; Squina, F.M.; Decker, S.R.; Prade, R.A. High-yield secretion of multiple client proteins in *Aspergillus*. *Enzym. Microb. Technol.* **2012**, *51*, 100–106. [[CrossRef](#)] [[PubMed](#)]
28. Higasi, P.M.; Velasco, J.A.; Pellegrini, V.O.; de Araújo, E.A.; França, B.A.; Keller, M.B.; Labate, C.A.; Blossom, B.M.; Segato, F.; Polikarpov, I. Light-stimulated T. thermophilus two-domain LPMO9H: Low-resolution SAXS model and synergy with cellulases. *Carbohydr. Polym.* **2021**, *260*, 117814. [[CrossRef](#)]
29. Sepulchro, A.G.V.; Pellegrini, V.O.; Dias, L.D.; Kadowaki, M.A.; Cannella, D.; Polikarpov, I. Combining pieces: A thorough analysis of light activation boosting power and co-substrate preferences for the catalytic efficiency of lytic polysaccharide monoxygenase MtLPMO9A. *Biofuel Res. J.* **2021**, *8*, 1454–1464. [[CrossRef](#)]
30. Keller, M.B.; Badino, S.F.; Blossom, B.M.; McBrayer, B.; Borch, K.; Westh, P. Promoting and Impeding Effects of Lytic Polysaccharide Monoxygenases on Glycoside Hydrolase Activity. *ACS Sustain. Chem. Eng.* **2020**, *8*, 14117–14126. [[CrossRef](#)]
31. Schüle, M. Enzymatic properties of cellulases from *Humicola insolens*. *J. Biotechnol.* **1997**, *57*, 71–81. [[CrossRef](#)]
32. Feng, X.; Ullah, N.; Wang, X.; Sun, X.; Li, C.; Bai, Y.; Chen, L.; Li, Z. Characterization of Bacterial Cellulose by *Gluconacetobacter hansenii* CGMCC 3917. *J. Food Sci.* **2015**, *80*, E2217–E2227. [[CrossRef](#)]
33. Frommhagen, M.; Koetsier, M.J.; Westphal, A.H.; Visser, J.; Hinz, S.W.A.; Vincken, J.-P.; van Berkel, W.J.H.; Kabel, M.A.; Gruppen, H. Lytic polysaccharide monoxygenases from *Myceliophthora thermophila* C1 differ in substrate preference and reducing agent specificity. *Biotechnol. Biofuels* **2016**, *9*, 186. [[CrossRef](#)]
34. Miller, G.L. Use of Dinitrosalicylic Acid Reagent for Determination of Reducing Sugar. *Anal. Chem.* **1959**, *31*, 426–428. [[CrossRef](#)]
35. Walton, P.H.; Davies, G.J. On the catalytic mechanisms of lytic polysaccharide monoxygenases. *Curr. Opin. Chem. Biol.* **2016**, *31*, 195–207. [[CrossRef](#)] [[PubMed](#)]
36. Monclaro, A.V.; Filho, E.X.F. Fungal lytic polysaccharide monoxygenases from family AA9: Recent developments and application in lignocellulose breakdown. *Int. J. Biol. Macromol.* **2017**, *102*, 771–778. [[CrossRef](#)] [[PubMed](#)]
37. Balajee, S.A.; Gribskov, J.L.; Hanley, E.; Nickle, D.; Marr, K.A. *Aspergillus lentulus* sp. nov., a New Sibling Species of *A. fumigatus*. *Eukaryot. Cell* **2005**, *4*, 625–632. [[CrossRef](#)] [[PubMed](#)]
38. Rokas, A.; Mead, M.E.; Steenwyk, J.L.; Oberlies, N.H.; Goldman, G.H. Evolving moldy murderers: *Aspergillus* section *Fumigati* as a model for studying the repeated evolution of fungal pathogenicity. *PLoS Pathog.* **2020**, *16*, e1008315. [[CrossRef](#)] [[PubMed](#)]

39. Rodrigues, K.B.; Macêdo, J.K.; Teixeira, T.; Barros, J.S.; Araújo, A.C.; Santos, F.P.; Quirino, B.F.; Brasil, B.S.; Salum, T.F.; Abdelnur, P.V.; et al. Recombinant expression of *Thermobifida fusca* E7 LPMO in *Pichia pastoris* and *Escherichia coli* and their functional characterization. *Carbohydr. Res.* **2017**, *448*, 175–181. [[CrossRef](#)]
40. Petrović, D.M.; Bissaro, B.; Chylenski, P.; Skaugen, M.; Sørli, M.; Jensen, M.S.; Aachmann, F.L.; Courtade, G.; Várnai, A.; Eijsink, V.G. Methylation of the N-terminal histidine protects a lytic polysaccharide monoxygenase from auto-oxidative inactivation. *Protein Sci.* **2018**, *27*, 1636–1650. [[CrossRef](#)]
41. Uchiyama, T.; Uchihashi, T.; Ishida, T.; Nakamura, A.; Vermaas, J.V.; Crowley, M.F.; Samejima, M.; Beckham, G.T.; Igarashi, K. Lytic polysaccharide monoxygenase increases cellobiohydrolases activity by promoting decrystallization of cellulose surface. *Sci. Adv.* **2022**, *8*, eade5155. [[CrossRef](#)]
42. Stepnov, A.A.; Christensen, I.A.; Forsberg, Z.; Aachmann, F.L.; Courtade, G.; Eijsink, V.G.H. The impact of reductants on the catalytic efficiency of a lytic polysaccharide monoxygenase and the special role of dehydroascorbic acid. *FEBS Lett.* **2021**, *596*, 53–70. [[CrossRef](#)]
43. Tölgo, M.; Hegnar, O.A.; Østby, H.; Várnai, A.; Vilaplana, F.; Eijsink, V.G.H.; Olsson, L. Comparison of Six Lytic Polysaccharide Monoxygenases from *Thermothielavioides terrestris* Shows That Functional Variation Underlies the Multiplicity of LPMO Genes in Filamentous Fungi. *Appl. Environ. Microbiol.* **2022**, *88*, e0009622. [[CrossRef](#)]
44. Golten, O.; Ayuso-Fernández, I.; Hall, K.R.; Stepnov, A.A.; Sørli, M.; Røhr, Å.K.; Eijsink, V.G.H. Reductants fuel lytic polysaccharide monoxygenase activity in a pH-dependent manner. *FEBS Lett.* **2023**, *597*, 1363–1374. [[CrossRef](#)]
45. Shen, J.; Griffiths, P.T.; Campbell, S.J.; Utinger, B.; Kalberer, M.; Paulson, S.E. Ascorbate oxidation by iron, copper and reactive oxygen species: Review, model development, and derivation of key rate constants. *Sci. Rep.* **2021**, *11*, 7417. [[CrossRef](#)] [[PubMed](#)]
46. Siegel, S.M.; Siegel, B.Z. Autoxidation of Pyrogallol: General Characteristics and Inhibition by Catalase. *Nature* **1958**, *181*, 1153–1154. [[CrossRef](#)] [[PubMed](#)]
47. Akagawa, M.; Shigemitsu, T.; Suyama, K. Production of Hydrogen Peroxide by Polyphenols and Polyphenol-rich Beverages under Quasi-physiological Conditions. *Biosci. Biotechnol. Biochem.* **2003**, *67*, 2632–2640. [[CrossRef](#)] [[PubMed](#)]
48. Li, X.; Beeson, W.T.; Phillips, C.M.; Marletta, M.A.; Cate, J.H. Structural basis for substrate targeting and catalysis by fungal polysaccharide monoxygenases. *Structure* **2012**, *20*, 1051–1061. [[CrossRef](#)]
49. Liu, B.; Kognole, A.A.; Wu, M.; Westereng, B.; Crowley, M.F.; Kim, S.; Dimarogona, M.; Payne, C.M.; Sandgren, M. Structural and molecular dynamics studies of a C1-oxidizing lytic polysaccharide monoxygenase from *Heterobasidion irregulare* reveal amino acids important for substrate recognition. *FEBS J.* **2018**, *285*, 2225–2242. [[CrossRef](#)]
50. Linder, M.; Nevanen, T.; Teeri, T.T. Design of a pH-dependent cellulose-binding domain. *FEBS Lett.* **1999**, *447*, 13–16. [[CrossRef](#)]
51. Calderaro, F.; Keser, M.; Akeroyd, M.; Bevers, L.E.; Eijsink, V.G.H.; Várnai, A.; Berg, M.A.v.D. Characterization of an AA9 LPMO from *Thielavia australiensis*, TausLPMO9B, under industrially relevant lignocellulose saccharification conditions. *Biotechnol. Biofuels* **2020**, *13*, 195. [[CrossRef](#)]
52. Alfani, F.; Gallifuoco, A.; Saporosi, A.; Spera, A.; Cantarella, M. Comparison of SHF and SSF processes for the bioconversion of steam-exploded wheat straw. *J. Ind. Microbiol. Biotechnol.* **2000**, *25*, 184–192. [[CrossRef](#)]
53. Kerkisick, C.; Willoughby, D. The Antioxidant Role of Glutathione and N-Acetyl-Cysteine Supplements and Exercise-Induced Oxidative Stress. *J. Int. Soc. Sports Nutr.* **2005**, *2*, 38–44. [[CrossRef](#)]
54. Kommedal, E.G.; Angeltveit, C.F.; Klau, L.J.; Ayuso-Fernández, I.; Arstad, B.; Antonsen, S.G.; Stenstrøm, Y.; Ekeberg, D.; Gírio, F.; Carvalheiro, F.; et al. Visible light-exposed lignin facilitates cellulose solubilization by lytic polysaccharide monoxygenases. *Nat. Commun.* **2023**, *14*, 1063. [[CrossRef](#)] [[PubMed](#)]
55. Müller, G.; Chylenski, P.; Bissaro, B.; Eijsink, V.G.H.; Horn, S.J. The impact of hydrogen peroxide supply on LPMO activity and overall saccharification efficiency of a commercial cellulase cocktail. *Biotechnol. Biofuels* **2018**, *11*, 209. [[CrossRef](#)] [[PubMed](#)]
56. Bissaro, B.; Røhr, Å.K.; Müller, G.; Chylenski, P.; Skaugen, M.; Forsberg, Z.; Horn, S.J.; Vaaje-Kolstad, G.; Eijsink, V.G.H. Oxidative cleavage of polysaccharides by monocopper enzymes depends on H₂O₂. *Nat. Chem. Biol.* **2017**, *13*, 1123–1128. [[CrossRef](#)] [[PubMed](#)]
57. Möllers, K.; Mikkelsen, H.; Simonsen, T.; Cannella, D.; Johansen, K.; Bjerrum, M.; Felby, C. On the formation and role of reactive oxygen species in light-driven LPMO oxidation of phosphoric acid swollen cellulose. *Carbohydr. Res.* **2017**, *448*, 182–186. [[CrossRef](#)] [[PubMed](#)]
58. Blossom, B.M.; Russo, D.A.; Singh, R.K.; van Oort, B.; Keller, M.B.; Simonsen, T.I.; Perzon, A.; Gamon, L.F.; Davies, M.J.; Cannella, D.; et al. Photobiocatalysis by a Lytic Polysaccharide Monoxygenase Using Intermittent Illumination. *ACS Sustain. Chem. Eng.* **2020**, *8*, 9301–9310. [[CrossRef](#)]
59. Bissaro, B.; Kommedal, E.; Røhr, Å.K.; Eijsink, V.G.H. Controlled depolymerization of cellulose by light-driven lytic polysaccharide oxygenases. *Nat. Commun.* **2020**, *11*, 890. [[CrossRef](#)]
60. Velasco, J.; Sepulchro, A.G.V.; Higasi, P.M.R.; Pellegrini, V.O.A.; Cannella, D.; de Oliveira, L.C.; Polikarpov, I.; Segato, F. Light Boosts the Activity of Novel LPMO from *Aspergillus fumigatus* Leading to Oxidative Cleavage of Cellulose and Hemicellulose. *ACS Sustain. Chem. Eng.* **2022**, *10*, 16969–16984. [[CrossRef](#)]
61. Kommedal, E.G.; Sæther, F.; Hahn, T.; Eijsink, V.G.H. Natural photoredox catalysts promote light-driven lytic polysaccharide monoxygenase reactions and enzymatic turnover of biomass. *Proc. Natl. Acad. Sci. USA* **2022**, *119*, e2204510119. [[CrossRef](#)]

62. Tokin, R.; Ipsen, J.; Westh, P.; Johansen, K.S. The synergy between LPMOs and cellulases in enzymatic saccharification of cellulose is both enzyme- and substrate-dependent. *Biotechnol. Lett.* **2020**, *42*, 1975–1984. [[CrossRef](#)]
63. Sagarika, M.S.; Parameswaran, C.; Senapati, A.; Barala, J.; Mitra, D.; Prabhukarthikeyan, S.; Kumar, A.; Nayak, A.K.; Panneerselvam, P. Lytic polysaccharide monoxygenases (LPMOs) producing microbes: A novel approach for rapid recycling of agricultural wastes. *Sci. Total Environ.* **2022**, *806*, 150451. [[CrossRef](#)]

Disclaimer/Publisher's Note: The statements, opinions and data contained in all publications are solely those of the individual author(s) and contributor(s) and not of MDPI and/or the editor(s). MDPI and/or the editor(s) disclaim responsibility for any injury to people or property resulting from any ideas, methods, instructions or products referred to in the content.